Enter: **OTC ASIA 2026**

Enter: Paper Number (OTC-36330-MS)

Fast-track Discovery To Development: Unified Ensemble Modeling as A Catalyst for Detailed Subsurface Uncertainty Quantification & Robust Field Development - A Case Study from Guyana Suriname Basin

Enter: M. Yasmin[1]*, R.M. Simamora[1], L.P. Lopez[1], H. Minhat[1], Z. Hasnan[1] D. Chakraborty[2], S. Ducroux[2], S. Strebelle[3], T.F. Munck[3], D. Sirat[3] , and P. Gautam[4]

[1] Petronas Carigali Sdn Bhd
[2,3] Halliburton
[4] Independent Consultant

Introduction

The offshore margins of Guyana, Suriname, and French Guyana (the "Guyanas Equatorial Margin") have become the focus of active hydrocarbon exploration over the last decade, with significant energy resources discovered since 2015 along both the Guyana and Suriname segments of the margin. Those discoveries are mainly associated with the Late Cretaceous series of the Guyana-Suriname Basin and they shed light to a rare situation where stratigraphic traps are particularly successful. The continental margin of Guyana and Suriname resulted from a complex geological history spanning a dual phase Mesozoic rifting and a post-rift phase influenced by Andean tectonism (at the origin of onshore drainage reorganization) and Caribbean plate tectonics Previous studies have shown that its sedimentary record constitutes a unique archive of the Mesozoic and Cenozoic tectono-stratigraphic evolution of the region (Sapin et al., 2016; Casson et al., 2021; Cronin et al., 2023).

Frontier deep-water basins such as the Guyana–Suriname Basin host significant hydrocarbon potential but are challenged by limited seismic bandwidth, sparse well control, loss of small-scale heterogeneity through upscaling, and linear, non-iterative project execution that extends exploration-to-development cycle times. Conventional 10–60 Hz seismic data commonly fail to resolve thin (5–15 m) turbidite sands and complex channel–lobe architectures, while traditional workflows impose sequential handovers between geoscience and engineering disciplines. This paper presents a modular, cyclic, uncertainty-centric workflow that enables a seamless exploration-to-development rollover within a unified environment. The workflow integrates (1) QC-driven seismic enhancement using Sparse Layer Inversion (SLI) and phase decomposition to extend bandwidth to 8–80 Hz and improve vertical resolution to approximately 7.5 m; (2) chrono-stratigraphy-anchored assisted horizon interpretation, extracting 18 third-order sequence boundaries over approximately 9,500 km²; (3) continuous, grid-less Scalable Earth Modeling (SEM) that preserves native well-log resolution (0.1 m) without averaging while co-simulating facies and petrophysical properties conditioned to seismic-derived trends/probabilities; (4) high-throughput probabilistic simulation, generating hundreds of calibrated static and dynamic models through ensemble based modeling spanning structural, facies, petrophysical, contact, SCAL, and PVT uncertainties and calibrated to DST data using an Ensemble Kalman Smoother; and (5) risk-weighted development planning, using Monte Carlo-derived connected-volume statistics and forecast envelopes (P0–P100 within ±15%) to optimize well placement and compare multi-well plateau strategies. Applied to a 9,500 km² 3D seismic survey and five wells, the workflow doubled stratigraphic resolution, delivered a regionally consistent geological framework, and cut the exploration-to-development lead time by >50% (≈18 months to ≈6 months). This replicable, data-fidelity-

preserving approach streamlines multidisciplinary integration, quantifies uncertainty, and supports decision-grade, risk-informed field development in complex frontier deep-water settings.

This paper presents a noble integrated, uncertainty-centric ensembled based workflow implemented from regional to field scale in the study area in the Guyana–Suriname deep-water Basin.

Keywords

Unified ensemble modeling, Grid-less geological modeling, Integrated static & dynamic uncertainties, Risk weighted field development, Sparse layer inversion, Fast-track exploration to development, Data driven modeling

Nomenclature

BHP = Bottom-Hole Pressure

DST = Drill Stem Test

FWL = Free-Water Level

GDE = Gross Depositional Environment

GWC = Gas–Water Contact

HM = History Matching

IRR = Internal Rate of Return

Kalman Smoother = Ensemble Kalman Smoother data assimilation algorithm

LST = Lowstand Systems Tract

MTD = Mass Transport Deposit

NPV = Net Present Value

P90, P50, P10 = Probabilistic percentiles representing low, median, and high outcomes

PI = Productivity Index

PVT = Pressure–Volume–Temperature

QC = Quality Control

RMS = Root Mean Square

SATNUM = Saturation Region Number

SCAL = Special Core Analysis

SEM = Scalable Earth Modeling

SLI = Sparse Layer Inversion

1. Introduction

Deep-water frontier basins continue to attract exploration and development interest due to the size and quality of recent discoveries; however, subsurface characterization in these settings remains challenging. Reservoirs are commonly composed of thin-bedded turbidite sands interbedded with mudstones and disrupted by mass transport deposits (MTDs), which are difficult to resolve with conventional seismic bandwidths. Sparse well control further compounds uncertainty in stratigraphic architecture, reservoir connectivity, and petrophysical distribution. As a result, traditional linear workflows—where seismic interpretation, geological modeling, and reservoir simulation are performed sequentially—often lead to long cycle times, late-stage rework, and overconfident base-case models that fail to capture uncertainty.

In recent years, advances in seismic bandwidth extension, assisted interpretation, and ensemble-based reservoir modeling have shown promise in addressing individual aspects of these challenges. Nevertheless, these methods are frequently applied in isolation, resulting in loss of data fidelity and limited feedback between disciplines. The Society of Petroleum Engineers (SPE) has increasingly emphasized uncertainty management, probabilistic forecasting, and integrated subsurface workflows as critical enablers for better decision-making.

This paper presents a field-scale application of an integrated, uncertainty-centric workflow implemented in the Guyana–Suriname deep-water Basin. The workflow explicitly treats reservoir modeling as an inverse problem and propagates geological and engineering uncertainty from seismic interpretation through development planning. The objectives of this study are to:

1. Improve seismic resolution and stratigraphic imaging of thin turbidite reservoirs using Sparse Layer Inversion (SLI).
2. Build a continuous, grid-less geological model that preserves native data resolution across exploration and development scales.
3. Quantify static and dynamic uncertainties through ensemble-based reservoir simulation calibrated with drill stem test (DST) data.
4. Demonstrate accelerated exploration-to-development transition (>50% time reduction) and risk-weighted planning in a frontier deep-water setting

2. Geological Setting

2.1 Regional Framework

The Guyana–Suriname Basin is a passive margin basin located offshore northeastern South America, bounded to the east by the Demerara Plateau and to the west by the Central Precambrian Shield. The basin evolved during Early Cretaceous rifting followed by post-rift thermal subsidence. During the Late Cretaceous (Campanian–Maastrichtian), sedimentation was dominated by deep-water gravity-flow systems sourced from the adjacent continental margin.

The Guyana Basin developed in response to Jurassic continental breakup associated with the opening of the North Atlantic Ocean, recording a complex interaction of extensional, transform, and magmatic tectonic processes along the northern margin of South America. The basin is characterized by strong along-strike variability in margin architecture, reflecting differences in plate kinematics, crustal inheritance, and magmatic input during rifting and early drift.

The basin margins exhibit multiple tectonic styles. To the east, along Suriname, the basin is bounded by the Demerara Plateau, which represents a passive extensional volcanic margin marked by significant magmatic addition during breakup. Moving westward toward the Guyana–Suriname border, the margin transitions into an oblique extensional setting, reflecting a combination of strike-slip and extensional deformation. Further west, offshore northwestern Guyana, the margin becomes predominantly transform in character, running subparallel to the present-day continental shelf. To the northeast, the basin is bounded by an ocean–ocean margin, which

evolved through time from an initially transform-dominated regime into one characterized by oblique extension as plate motions reorganized *(Trude et al. (2022b))*.

Plate reconstruction models indicate that rifting and early seafloor spreading initiated under an NNW–SSE extensional stress regime between approximately 190 and 160 Ma. During this early phase, extension was accommodated by segmented rift systems and localized magmatism. Subsequently, relative plate motion rotated to a NW–SE orientation, fundamentally altering the style of deformation and contributing to the development of transform and oblique margin segments. This change in kinematics exerted first-order control on basin geometry, crustal thinning patterns, and sediment pathways *(Trude et al. (2022b))*.

Water depths in the study area range from approximately 1,500 to 3,000 m. Reservoir targets consist primarily of submarine channel, levee, and lobe deposits interbedded with hemipelagic mudstones and affected by slope instability processes.

2.2 *Depositional Evolution*

The Suriname Basin developed during the Early to Middle Jurassic following emplacement of a voluminous Early Jurassic volcanic succession related to activity of the Sierra Leone (Bahamas) hotspot (Phase 1). This localized magmatism exerted a first-order control on margin segmentation, resulting in contrasting tectonic architectures: a volcanic passive margin along the western margin of the Demerara Plateau and a transform margin developed along the Guyana sector to the west. During Phase 2, a mixed clastic–carbonate platform system was established from the Late Jurassic through the Early Cretaceous. Platform growth was dominated by aggradational stacking patterns, indicating sustained accommodation creation until the Early Aptian. Phase 3 records a shift to retrogradational platform evolution, with pronounced backstepping culminating during the Cenomanian–Turonian transition, coeval with regionally extensive deposition of organic-rich marine shales. This long-term transgressive evolution proceeded through several discrete flooding episodes, including late Early Aptian flooding followed by renewed progradation, Early Albian flooding, Late Albian to Cenomanian flooding above the breakup unconformity, and maximum platform retreat at the Cenomanian–Turonian boundary. The composite stratigraphic response reflects the interaction of long-term eustatic sea-level rise, increased thermal subsidence following Aptian–Albian Equatorial Atlantic opening, and relatively low sediment supply to the evolving margin (Delhaye-Prat et al. 2024)

3. Workflow Overview

The integrated workflow implemented for this study is described below

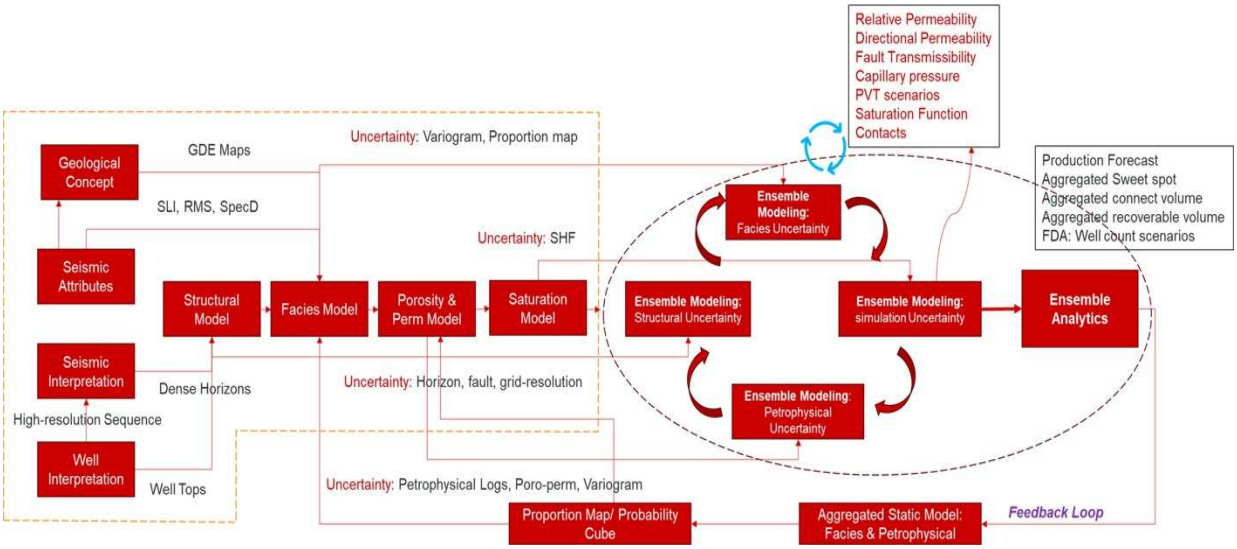

Figure 1: Illustrates the integrated exploration to field development cyclic workflow under the umbrella of uncertainty

3.1 Depositional Element Mapping & Regional Context:

Based on regional depositional element (GDE) mapping and chrono-stratigraphic correlation, three main depositional phases were identified within the Campanian interval:

- **Early Campanian (K190 LST):** The Early Campanian K190 Lowstand Systems Tract is dominated by slope-bypass depositional systems, reflecting a period of relative sea-level fall and reduced accommodation along the continental margin. Sediment supply is dominantly point-sourced through the Berbice Canyon, resulting in a pronounced sediment bypass zone across the Suriname shelf (Figure 3). Sedimentation during this interval is characterized by the development of narrow, deeply incised, and locally erosive slope channels that acted primarily as conduits for sediment transfer from the shelf edge to the basin floor, with limited sediment retention along the slope. Channel fills are typically thin, laterally restricted, and commonly composed of amalgamated sand-prone facies, indicating high-energy, gravity-driven flows. Mass-transport deposits (MTDs) are volumetrically minor and discontinuous, suggesting relatively stable slope conditions, limited oversteepening, and low rates of slope failure during this phase. The overall depositional architecture indicates efficient sediment bypass across the slope, minimal aggradation, and weak development of slope aprons or levee complexes, consistent with a bypass-dominated lowstand regime.

- **Middle Campanian (K200 LST):** Lowstand systems tract characterized by development of stacked intra-slope channel complexes, reflecting increased sediment supply and efficient sediment bypass across the slope (Figure 4). Development of point-sourced, channelized depositional systems across both the Guyana and Suriname slopes, accompanied by an overall increase in sediment flux. Channel bodies display vertical stacking and lateral amalgamation, indicating repeated incision and reoccupation of established sediment fairways during relative sea-level lowstand. This interval records the first significant occurrence of slumps and mass-transport deposits (MTDs), associated with slope oversteepening and instability driven by elevated sedimentation rates and rapid sediment loading.

- **Late Campanian to Early Maastrichtian (K210 LST):** This interval is characterized by lowstand deposition dominated by line-sourced submarine apron systems and widespread mass-transport processes. A line-sourced depositional system developed across the Suriname shelf, with mass-transport deposits becoming increasingly dominant as the intra-slope environment underwent progressive destabilization (Figure 5). Sedimentation was controlled by repeated slope instability, resulting in extensive slump sheets, debrites, and slide complexes that locally amalgamate into composite mass-transport deposits (MTDs). These gravity-driven deposits preferentially infilled and re-occupied pre-existing erosional depressions and slope gullies, which acted as conduits for subsequent turbidity currents. Turbidite flows, sourced from updip shelf-edge and upper-slope failures, locally ponded within these bathymetric lows, forming discontinuous sand-prone bodies interbedded with chaotic to semi-coherent MTDs. The overall depositional architecture reflects a strongly bypass-dominated slope system under lowstand conditions, with sediment routing focused along linear slope segments rather than discrete point-fed channels.

These depositional trends provided the geological framework for seismic interpretation and reservoir modeling.

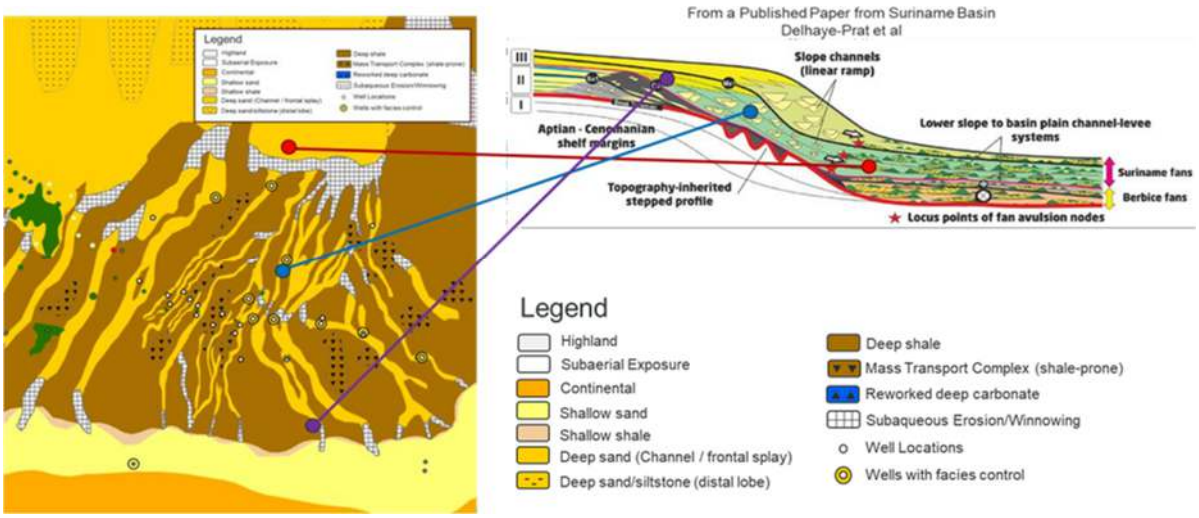

Figure 2: Depositional Setting of the Study Area

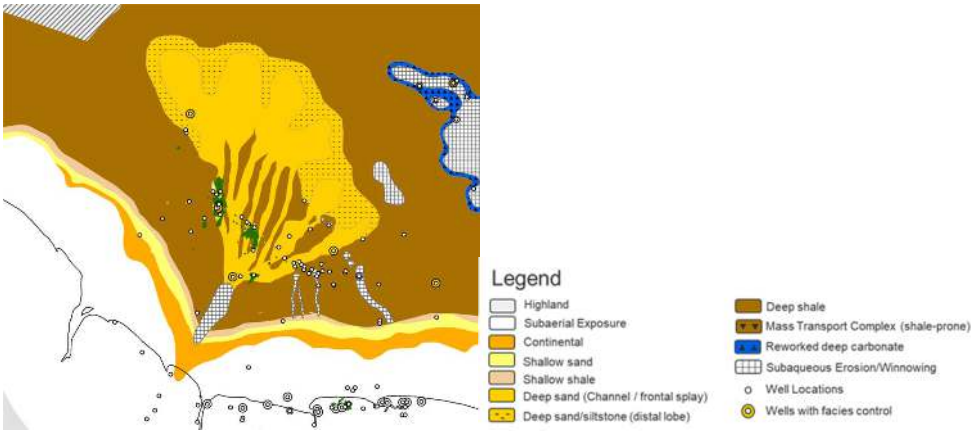

Figure 3: Late Santonian-Early Campanian (K190 LST)

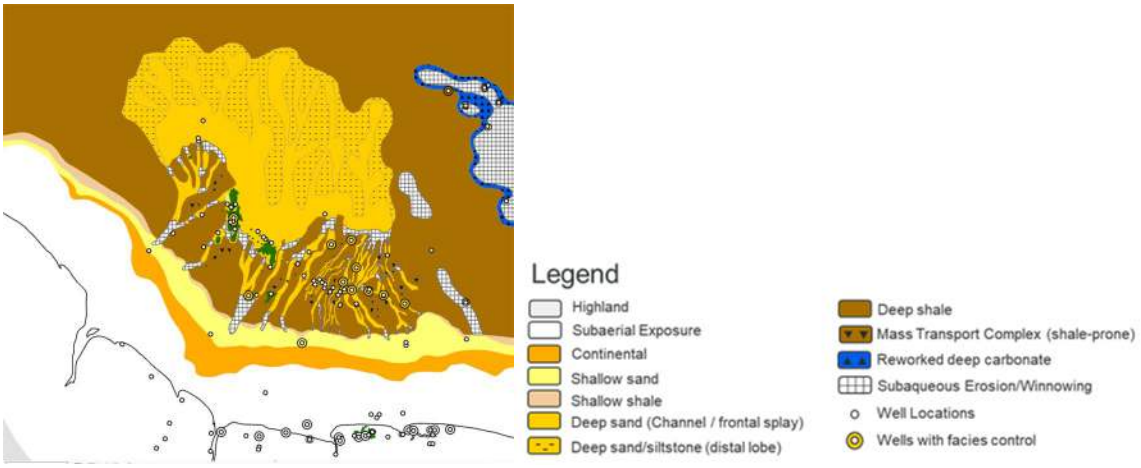

Figure 4: Early-Middle Campanian (K200 LST)

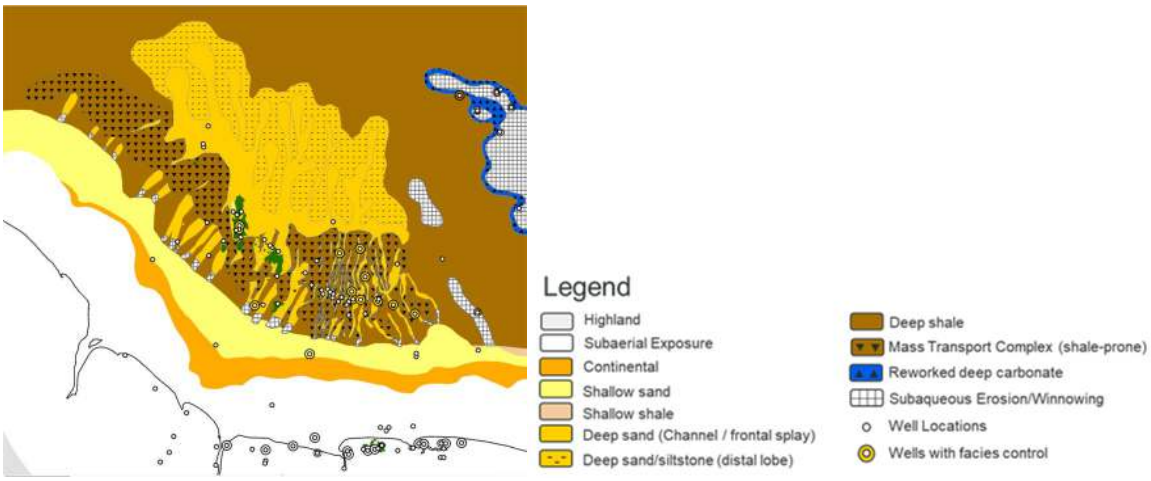

Figure 5:Late Campanian-Early Maastrichtian (K210 LST)

3.2 Sparse Layer Inversion (SLI):

Sparse Layer Inversion (SLI) was implemented within a stratigraphically constrained framework derived from GDE-based facies interpretation. Zero Phase conversion was applied prior to Sparse Layer Inversion to recover to make the Seismic volume consistent phase at the zone of interest and mitigate wavelet phase uncertainty, thereby enabling a more robust separation of overlapping reflection events.

The combined SLI workflow effectively extended the usable seismic bandwidth from approximately 10–40 Hz in the pre-inversion data to about 5–80 Hz in the SLI inverted volumes. This bandwidth enhancement translated to a significant improvement in vertical resolution, achieving an effective resolvability of approximately 8-10 m, which is critical for resolving thin-bedded reservoir and nonreservoir facies. The inversion results were generated through an iterative process in which spectral shaping, wavelet estimation, and model updating were repeatedly refined to ensure consistency with both seismic data and the geological framework.

Quality control (QC) was embedded at each iteration using quantitative and geologically driven metrics . Horizon and well tie-point misfits were monitored to evaluate and confirm extra layer (reflection) and phase alignment, The iterative QC ensures the best fit parameterization metrics with geological alignments ensured that the final SLI products were both seismically coherent and geologically consistent, providing a reliable input for subsequent reservoir characterization and modeling workflows.

3.3 Gridless Earth Model/Scalable Earh Model (SEM):

A multi-purpose, multi-scale shared earth model was constructed using a grid-less modeling approach that preserves the native resolution of the input data. All well-log measurements were honored at their original sampling interval (typically 0.1 m), with no vertical averaging or numerical upscaling applied during model construction. This approach ensures that fine-scale stratigraphic and petrophysical variability observed in the wells is retained and propagated consistently across the model domain.

Facies and petrophysical properties were co-simulated within the same grid-less framework to explicitly preserve small-scale heterogeneities and their spatial relationships. The co-simulation workflow generates continuous facies probability volumes and property realizations that are internally consistent and conditioned to available well and seismic-derived constraints. Resulting facies probability distributions and connectivity metrics (e.g., net-connected thickness and lateral continuity indicators) were established directly from the SEM model conform with the Well test data (e.g., DST). These quantitative measures were then used to iteratively inform geological

interpretation, assess uncertainty, and provide robust inputs to dynamic simulation and development planning, without the loss of information typically associated with conventional grid-based upscaling.

3.4 Ensembled Based Uncertainty-Centric Ensemble Simulation & Development Planning:

An ensemble-based, uncertainty-centric workflow was implemented to support integrated reservoir simulation and development planning. Key static and dynamic uncertainties were explicitly quantified and propagated through the modeling chain using a structured experimental design. Structural model and the Facies proportions/probability volumes from the gridles static modeling are used. Facies Static uncertainties included facies proportion variability (±10% relative perturbation around the base-case proportions) and porosity distribution uncertainty, while dynamic uncertainties focused on relative permeability endpoint variations (±0.05 on normalized endpoints). These uncertainties were sampled using a Latin Hypercube Sampling (LHS) scheme to ensure efficient and statistically representative coverage of the multidimensional uncertainty space. A total of 100 geologically consistent realizations were generated. Dynamic calibration incorporated pressure and rate data, including constraints derived from Drill Stem Test (DST) measurements, to reduce non-uniqueness and improve the physical realism of flow responses. This iterative calibration ensured consistency between static geological realizations and dynamic reservoir performance.

The resulting ensemble of history-matched models was used to evaluate development scenarios in a probabilistic framework. Production forecasts from all realizations were aggregated to quantify uncertainty envelopes on key performance indicators. Economic evaluations were conducted on a realization-by-realization basis and subsequently combined to derive risk-weighted metrics. Development options were ranked using a multi-objective decision framework that balances expected Net Present Value (NPV), Internal Rate of Return (IRR), and downside risk quantified through Value-at-Risk (VaR). This approach enabled objective comparison of alternative multi-well development strategies while explicitly accounting for subsurface uncertainty and economic risk.

4. Method

4.1 Defining the 3rd -4th Order sequence boundaries at wells using the stratigraphic framework and automating the horizon interpretation using ML driven approach throughout ~9500 SQKM

Based on the following interval/key sequences 18 horizons were interpreted from seabed to basement using the ML driven approach. The ML driven dense horizon interpretation is focused on the following key stratigraphic interval.

Interval	**Key sequence picks & chrono-stratigraphy**	**Depositional setting**
Early Campanian (Figure 3)	Late Santonian-Early Campanian (K190 LST)	**Slope-bypass domain.** Sediment delivered through the Berbice Canyon as point-sourced, erosive turbidity currents. Seismic GDE map shows narrow channel–lobe fairways, minimal mass-transport deposits (MTDs)
Middle Campanian (Figure 4)	Earl- Middle Campanian (K200 LST)	**Intra-slope stacked channels.** Increased sediment flux builds multi-story channel complexes; first appearance of slump/MTD incision as slope instability rises
Late Campanian (Figure 5)	Late Campanian-Early Maastrichtian (K210 LST)	**Line-sourced apron & mass-transport dominated.** Shelf-edge failure produces extensive slump/MTD sheets that

		onlap earlier channels; turbidite flows re-occupy depressions creating stacked, laterally migrating channels

Table 1:Key Chronostratigraphic Interval and Depositional Setting of the study area

Local (Delhaye-Prat et al. 2024) and regional analogs from the Equatorial Atlantic margins (e.g., Congo and Santos basins) demonstrate similar depositional architectures and MTD influences, validating the applicability of sequence stratigraphy and depositional element frameworks for reservoir characterization in this setting.

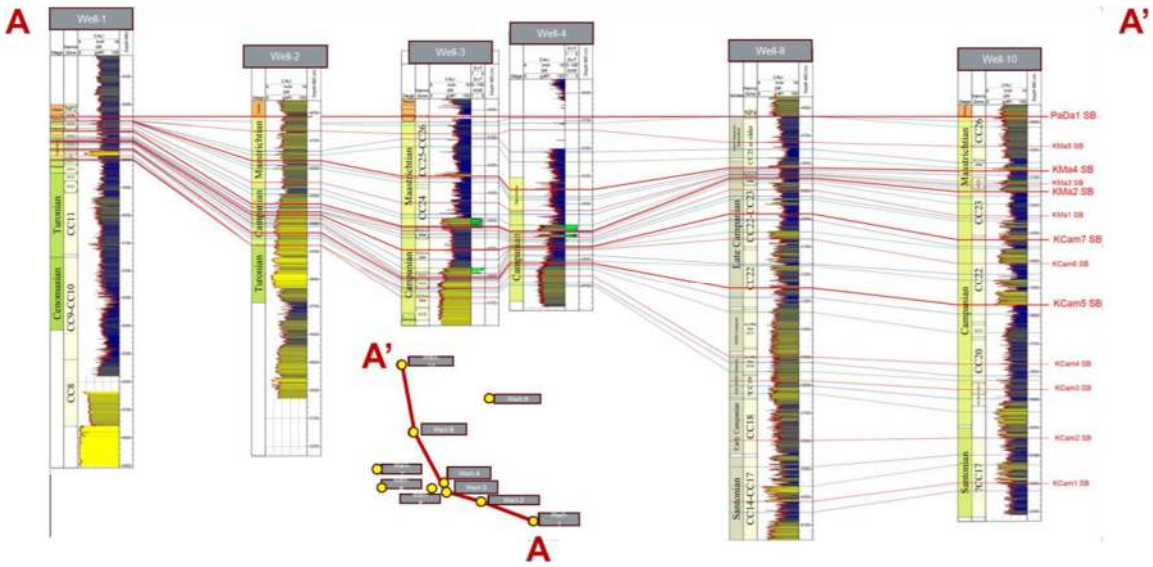

Figure 6:Sequence boundaries with regional seismic expression highlighted in dark red

Leveraging the chronostratigraphic framework (GTS2020) and GDE facies templates, automated horizon picking extracted 18 consistent layer interpretations through ML driven Assisted Horizon Interpretation approach. Horizon picks were validated against well tops and GDE facies transitions, achieving <20 m tie errors and ensuring consistent stratigraphic layering across channels, lobes, and MTD-influenced zones.

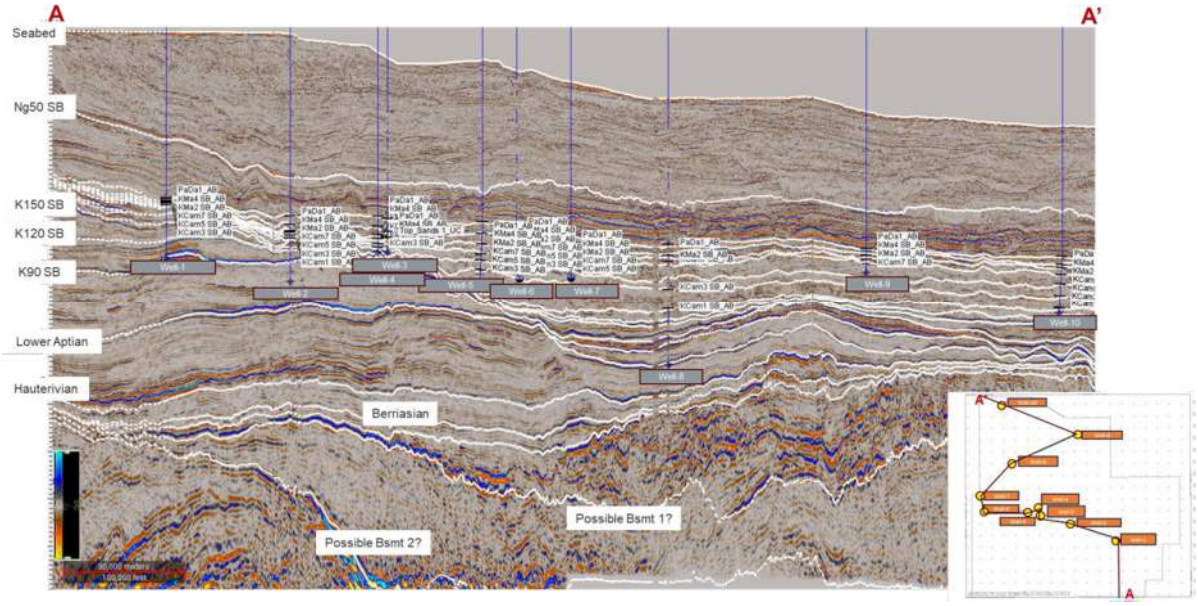

Figure 7:Cross section through the depth seismic volume, passing through the 10 key wells that were utilized

4.2 Defining High resolution seismic at the prospect level for better stratigraphic architecture and facies trend delineation at the reservoir level

The Sparse Layer Inversion (SLI) as demonstrated in Figure 8 and Figure 9 has the required potential to uncover the hidden reservoir features that can impact productivity or well performance with further improvement in the prediction of reservoir properties and reserves and finally helps in optimizing well placement with better understanding of deposition and connectivity.

The key steps need to be taken before implementing the Sparse Layer Inversion involves:

- Seismic Data Conditioning
- Seismic Wavelet phase Calculation and zero phase conversion of Seismic data
- Edge filtering structural filters
- Parameterization and running Sparse layer algorithm using Dipole decomposition.

Sparse Layer Inversion (SLI) is a high-resolution inversion technique for seismic data. It transforms standard bandwidth data with a prominent peak frequency into high-resolution data with a broader bandwidth, where the bandwidth extension is user-defined. However, this transformation is non-unique, especially at higher frequencies. SLI does not rely on well logs as an initial model and operates on a trace-by-trace basis without spatial constraints. Well data is later used to calibrate and validate the results by constraining the frequency.

SLI is an amplitude-preserving process, making it ideal for high-resolution seismic data analysis, attribute calculation, and quantitative workflows, such as conventional seismic inversion. It can also be applied to multiple partial stacks to create high-resolution gathers for Amplitude Versus Offset (AVO) analysis and pre-stack inversion work.

In this project, the results from SLI were further used as inputs for high-resolution sequence stratigraphic interpretation and used as a guidance/trend for geostatistics-based griddles/Scalable reservoir distribution modeling.

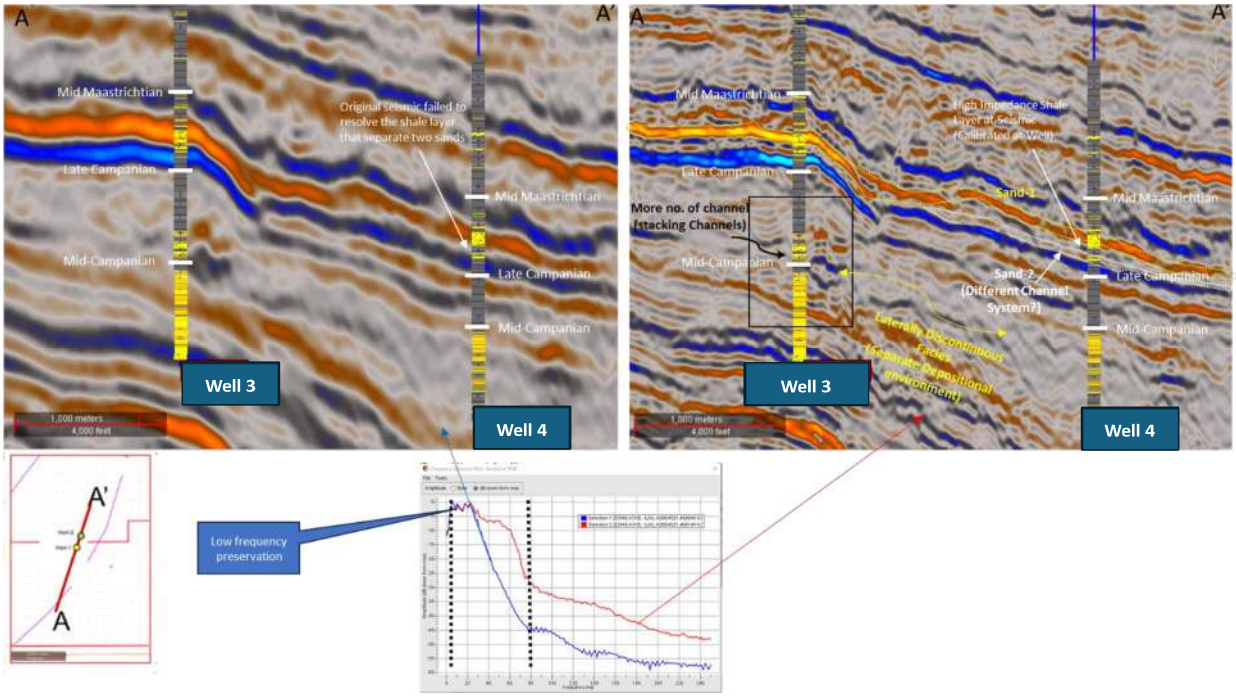

Figure 8:Comparison between original seismic and high resolutions seismic from sparse layer inversion

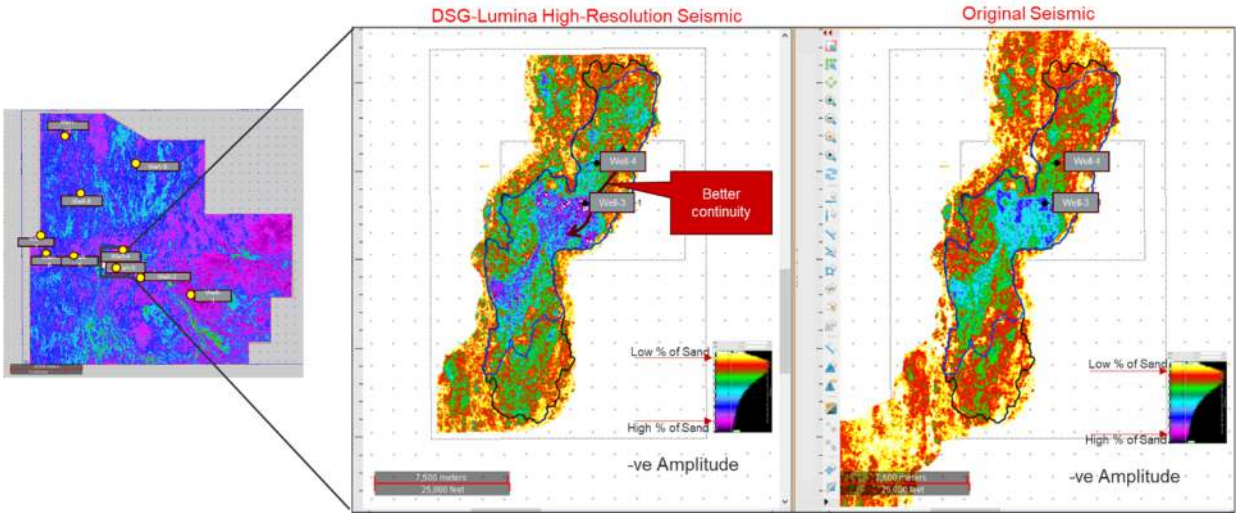

Figure 9:Better sand continuity captured in the high-resolution sparse layer inversion seismic amplitude compared to original seismic amplitude.

4.3 Single Consistent Regional to Reservoir level Grid-less Model

The results from advanced quantitative workflows have been integrated into the sub-surface geostatistical model. The biggest differentiating components of this modeling solution is dynamic scaling which provides the provision to the geo-modelers do both upscaling and downscaling of the resolution as per the project objective and requirement. This grid-less modeling has an inherent benefit of not locking the resolution model as based on the decision-making process additional points can be added to the model which gets recomputed by the geostatistical model.

In this project, in the attempt of using this model for multi-purpose scenarios, the scalability factor has been introduced to build a larger extent model including the potential near field leads/prospects into the same model without compromising on the resolution of the model. The model covers major discoveries and potential near field prospects across region with static volumetric extracted from the high-resolution model zoomed in from the integrated "Shared Earth Container" grid-less model (Figure 10)

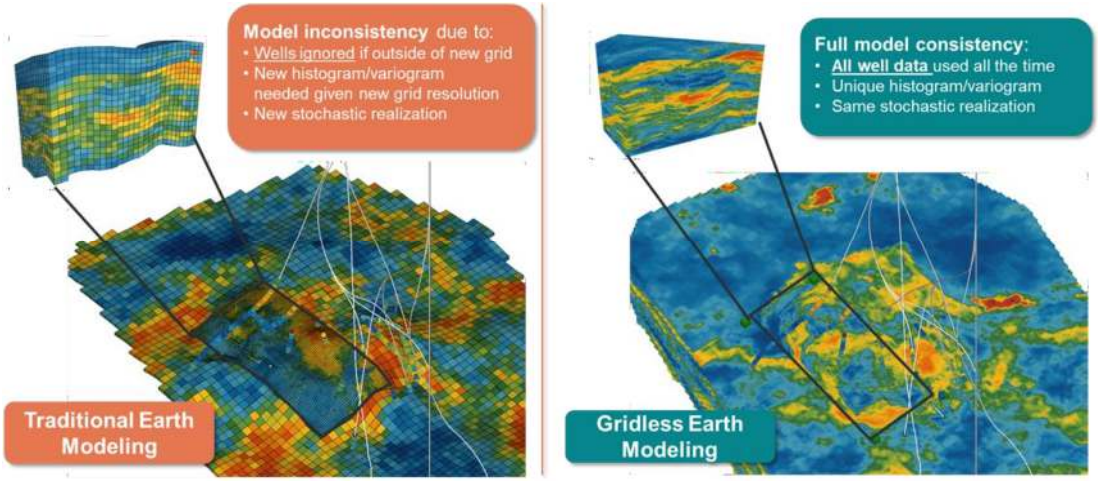

Figure 10:Comparison between grid-based model and grid-less model (a reference picture not from the study)

Well logs and seismic facies trends along with regional GDE maps were analyzed for variogram ranges to build the grid-less facies model for the regional scale. Fine scale facies architecture was generated using high resolution seismic inversion approach for one of the three prospects part of the regional scale grid-less model (***Figure 11***). We preserved full vertical and lateral detail as data was used at its original resolution. Porosity, permeability (***Figure 12***) were co-simulated, and facies (sandstone, siltstone, mudstone, conglomerate, and carbonate) were generated using pluri-gaussian algorithm. Cross-covariance functions derived from empirical semi-variograms ensure preservation of multivariate relationships across scales. Directional search ellipsoids, defined from geometric analyses of facies bodies, enforce anisotropy in channel and bedform orientations, capturing depositional trends without averaging or upscaling. Soft conditioning uses seismic-derived facies probability volumes (***Figure 12***) to guide co-simulation, aligning fine-scale well-log heterogeneities with regional depositional patterns.

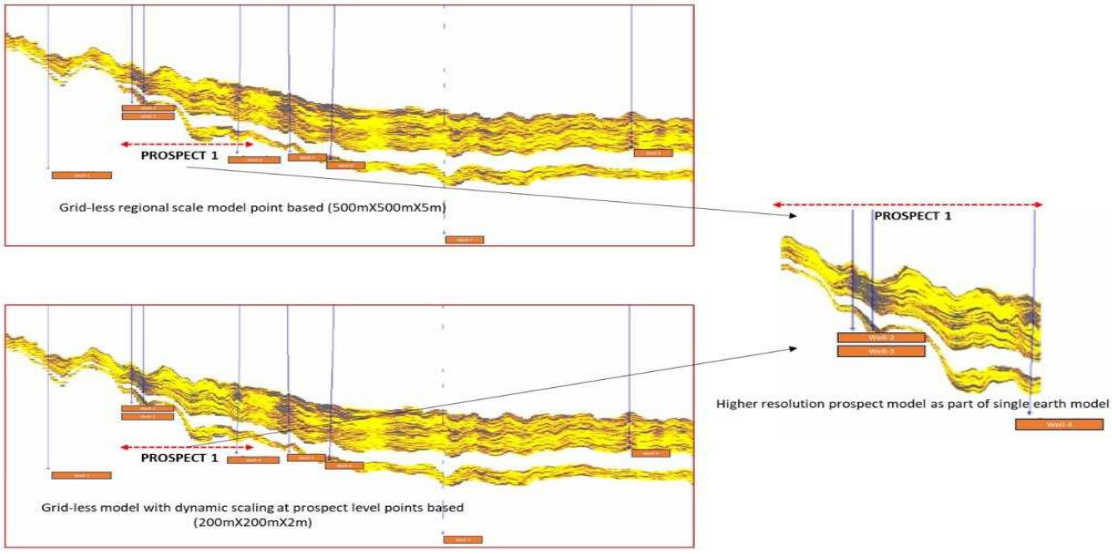

Figure 11:Shared grid-less earth model with dynamic scaling from coarser to finer resolution highlighting two different resolutions within the same geological model

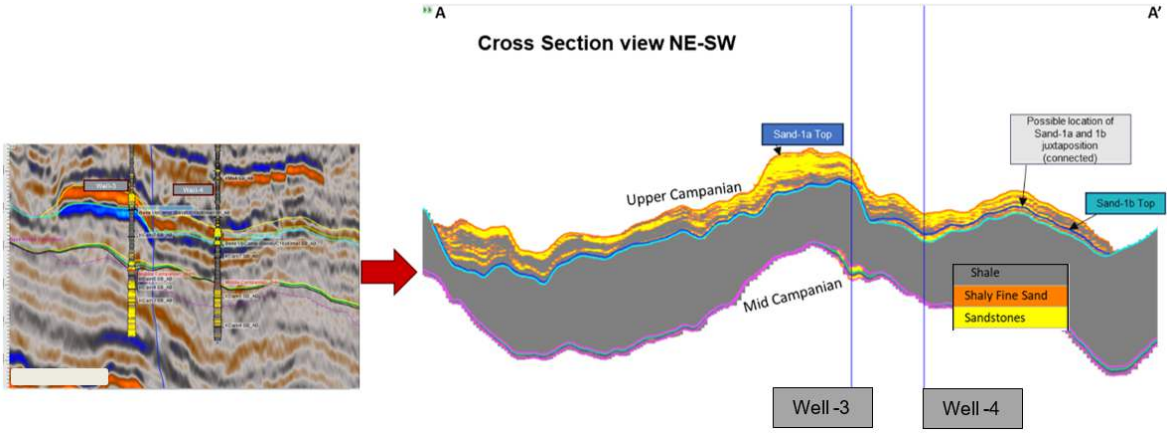

Figure 12:Grid-less facies model conditioned to facies trend generated from high resolutions seismic

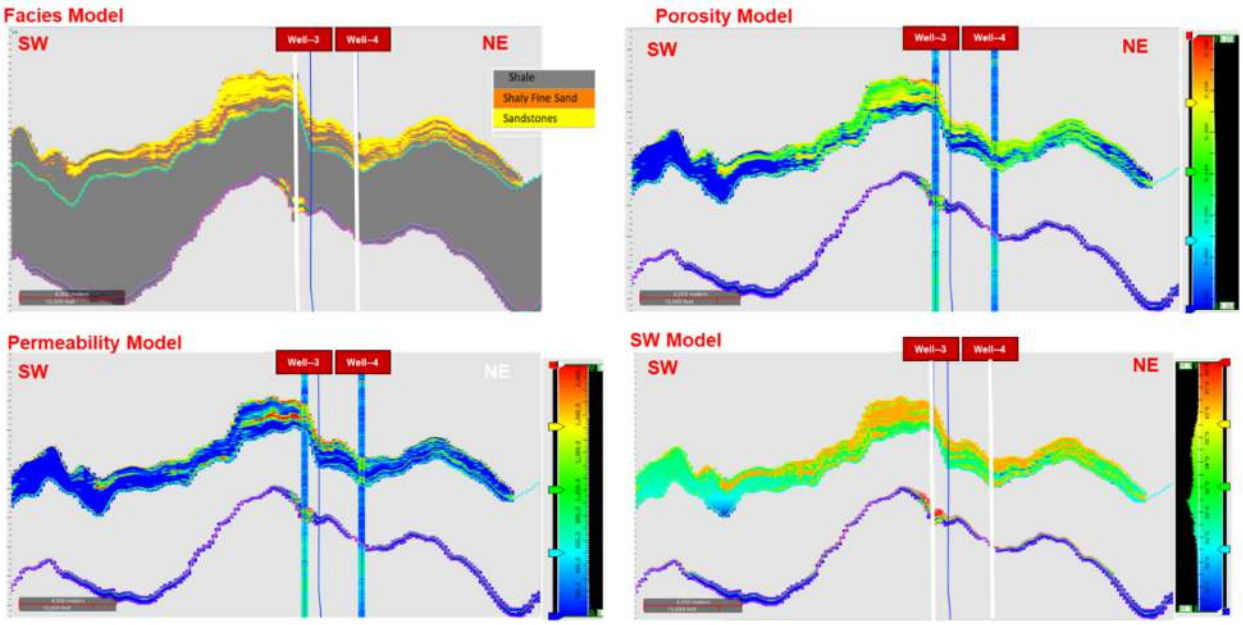

Figure 13:Grid-less facies and petrophysical models

4.4 Uncertainty-Based Unified Ensemble Modelling

Conventional reservoir-modeling workflows have historically emphasized the construction of a single most-likely ("base case") representation of the subsurface, integrating interpretations of structure, facies architecture, petrophysical properties, and fluid behavior into a so-called best technical case model. Significant time and computational effort are typically invested in building and maintaining this deterministic representation. However, as new static or dynamic data become available, the best technical case often requires substantial revision or complete reconstruction. Moreover, at later stages of field development, pronounced mismatches frequently emerge between observed dynamic responses (e.g., pressure and production data) and model forecasts.

Traditional history-matching practices generally attempt to reduce these mismatches by adjusting a limited subset of model parameters—commonly petrophysical properties such as porosity or permeability through the application of multipliers—while other critical components, including structural geometry, stratigraphic architecture, and facies distribution, remain largely unchanged. This selective updating leads to biased models that inadequately represent subsurface uncertainty and ultimately compromises the reliability of production forecasts and development planning.

This study introduces a fundamentally different paradigm in which reservoir modeling is formulated as an inverse problem. In this framework, reservoir data are interpreted as indirect observations of uncertain subsurface properties, each characterized by significant uncertainty. To consistently honor these uncertainties, we propose a probabilistic methodology referred to as Unified Ensemble Modelling. The approach constructs an ensemble of equiprobable reservoir models in which all key subsurface components are described by probability distributions rather than single deterministic realizations. This ensemble-based representation enables robust uncertainty quantification, improved risk assessment, and more informed optimization of reservoir development and management decisions.

4.4.1 Change in Mindset and Embracing the Uncertainties:

Ensemble modeling starts with the definition of the ranges for the subsurface uncertainties associated with the previously defined geological concept. Refer to Table 2: Static uncertainties and Table 3:Dynamic uncertainties for the complete list of uncertainties considered in this project.

Domain	**Range / Strategy**	**Rationale**
Structural framework (horizon depths, fault throws)	Multiple realizations spanning tens of meters vertically and proportionate lateral shifts	Accounts for misties, depth- conversion errors, and sparse velocity control
Facies architecture & trend maps	Alternative regional trend maps and sand-proportion cases (low / base / high)	Reflects uncertainty in depositional element interpretation and sand–shale ratio
Petrophysical distributions (porosity, permeability)	P10 – P90 envelopes co- simulated at native 0.1 m log resolution	Preserves well-log heterogeneity while bracketing uncertainty in histograms
Spatial continuity (variogram ranges, anisotropy)	"Short", "base", and "long" continuity scenarios with alternative anisotropy ratios	Captures uncertainty in lateral connectivity of channels and levees
Fluid contacts (GWC / FWL depths)	Vertical windows of several ten meters per reservoir unit	Encompasses scatter in pressure and resistivity break points

Table 2: Static uncertainties

Domain	**Range / Strategy**	**Rationale**
Relative-permeability (SCAL) curves	End-member sets per facies (high-mobility ↔ low-mobility)	Brackets uncertainty in multiphase flow behaviour
PVT & fluid properties (μ, ρ, cf)	Samples drawn from Drill Stem Test (DST)–derived envelopes	Propagates variability in in-situ fluid response
Well & completion factors (skin, PI, tubing limits)	Low-restriction ↔ high-restriction cases within production scenarios	Captures uncertainty in mechanical performance and damage
Fault transmissibility / sealing	Fully sealing ↔ fully open, plus intermediate leak cases	Tests sensitivity of compartmentalization and pressure support
Development strategies (well count, plateau targets)	5- vs 7-well blueprints; conservative vs aggressive plateaus	Reflects operational choices and economic trade-offs

Table 3:Dynamic uncertainties

These uncertainties include the depth of the interpreted horizons (**Figure *14***), considering the ambiguities of seismic interpretation and the uncertainties inherent to the velocity model.

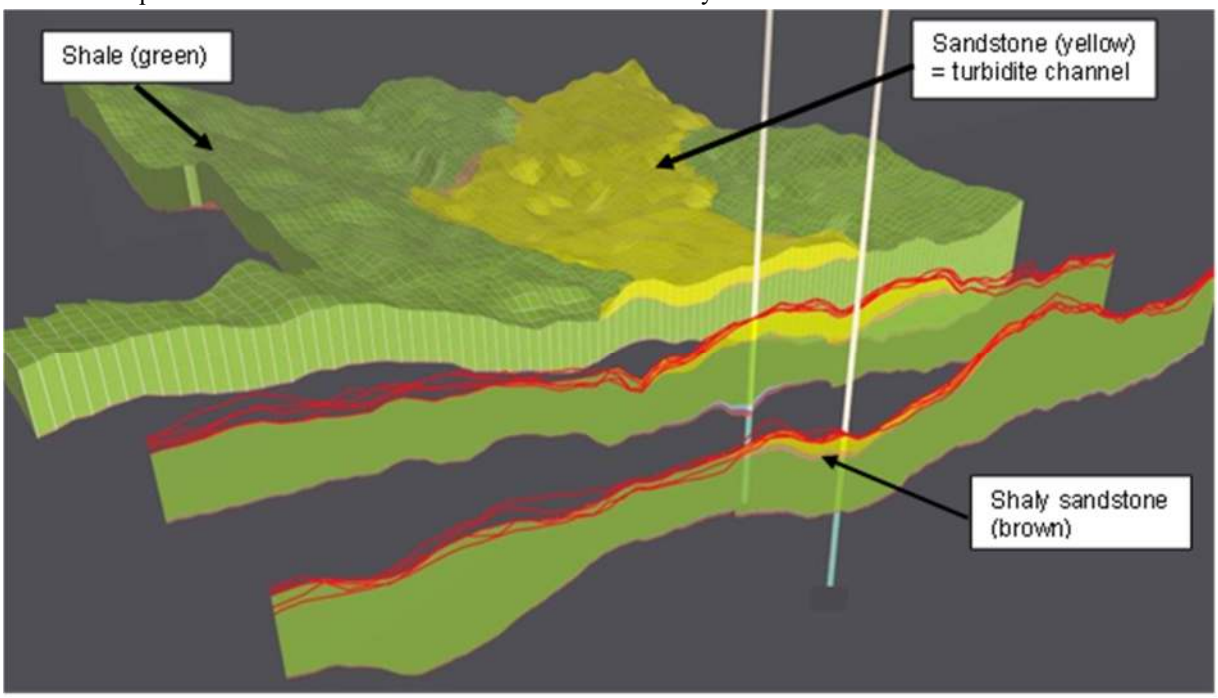

Figure 14:Horizon uncertainty highlighted in red (each line represents a possible top surface for the reservoir), using the Bayesian approach for structural variability

The reservoir uncertainties also consist of the facies proportions and property histograms inferred from the well log data, as well as the variograms, and the correlation between porosity and permeability. An ensemble of one hundred physical static and dynamic models were generated for calibration to available DST data. Figure 15 below highlights facies and permeability, giving a glimpse of the number of models generated and the variability in the ensemble.

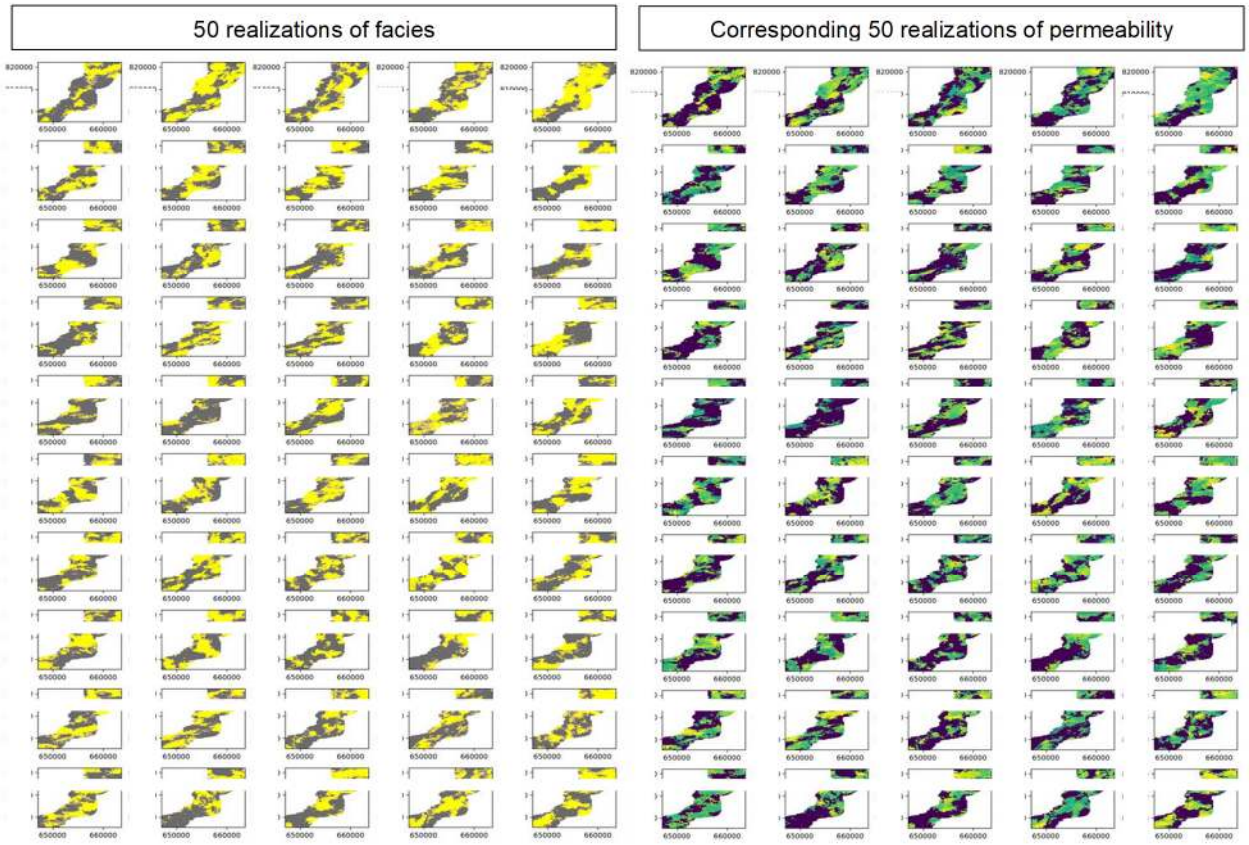

Figure 15:Figure 13: 50 representations (out of 100 in entire ensemble) of plausible facies models (Left side – Yellow = Sand; Grey = Shale) and permeability models (Right side – color Scale follows facies model with higher perm in the Sandstone)

An initial ensemble of models is created by randomly drawing parameter values within the previously defined uncertainty boundaries and automatically building the corresponding reservoir models. This step also samples additional uncertainties in dynamic model characterization, such as PVT and relative permeability parameters. In this example, each facies was assigned a different saturation region number (SATNUM) and corresponding range for Corey coefficients and end-points uncertainty parameters: SATNUM=1 for Shale, SATNUM = 2 for Shaly/Fine Sand and SATNUM = 3 for Sand (See Figure 16).

Sand (SATNUM=3)

Sat Num Code	Property	Distribution	Mean	Std...	Min	Max	Unit	Dependent Property	Correlation Coefficient
3	Sw Min	Normal	0.18	0.1	0.05	0.3	Dimensionless	None	None
3	Sgcr	Normal	0.1	0.03	0.05	0.18	Dimensionless	None	None
3	Gas Exponent	Normal	2.3	0.25	1.8	2.8	Dimensionless	None	None
3	Krg At Sw Min	Normal	0.8	0.05	0.7	0.9	Dimensionless	None	None
3	Swcr	Normal	0.185	0.068	0.05	0.32	Dimensionless	Sw Min	Linear Positive
3	Water Exponent	Normal	4.65	0.425	3.8	5.5	Dimensionless	None	None
3	Krw At Sorw	Normal	0.275	0.037	0.2	0.35	Dimensionless	None	None
3	Krw At Sw One	Constant	0.35				Dimensionless	None	None

Fine Sand (SATNUM=2)

Sat Num Code	Property	Distribution	Mean	Std...	Min	Max	Unit	Dependent Property	Correlation Coefficient
2	Sw Min	Normal	0.3	0.05	0.2	0.4	Dimensionless	None	None
2	Sgcr	Normal	0.1	0.03	0.05	0.18	Dimensionless	None	None
2	Gas Exponent	Normal	2.3	0.25	1.8	2.8	Dimensionless	None	None
2	Krg At Sw Min	Normal	0.8	0.05	0.7	0.9	Dimensionless	None	None
2	Swcr	Normal	0.31	0.068	0.21	0.41	Dimensionless	Sw Min	Linear Positive
2	Water Exponent	Normal	4.65	0.425	3.8	5.5	Dimensionless	None	None
2	Krw At Sorw	Normal	0.275	0.037	0.2	0.35	Dimensionless	None	None
2	Krw At Sw One	Constant	0.35				Dimensionless	None	None

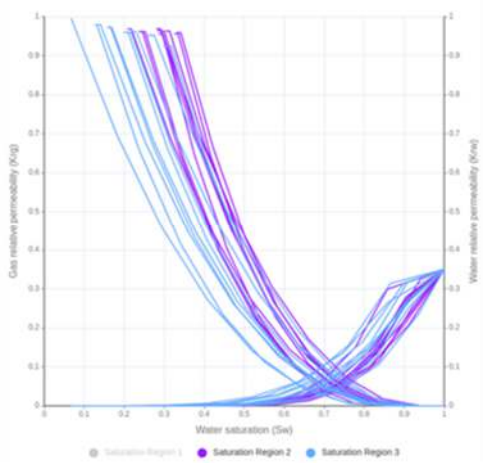

Figure 16:Relative permeability uncertainty set up for sand and shaly sand facies

Flow simulating the resulting initial ensemble makes it possible to check if the corresponding simulations bracket the actual production history (Figure 17).

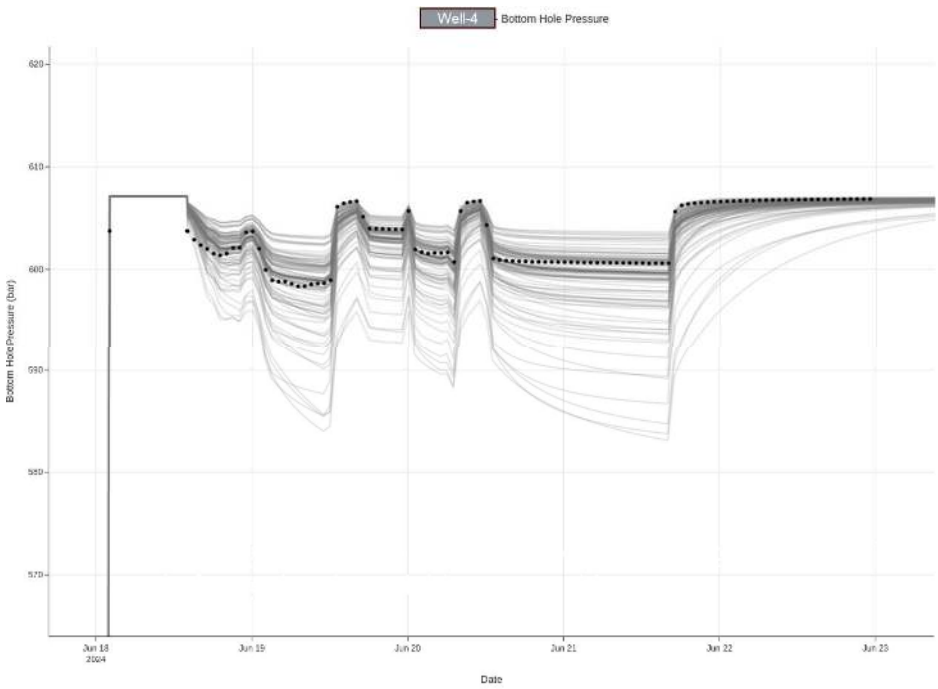

Figure 17:DST pressure response (Black dots) bracketed by initial ensemble members (grey lines) given the range of static and dynamic uncertainties

If the ensemble of cases do not cover the observed data, the geological concept and/or the subsurface uncertainty boundaries may need to be refined, resulting in a new ensemble. This iterative process can be accelerated through a fit-for- purpose modelling approach, using simple geological scenarios first (e.g., will two facies be sufficient

to capture flow dynamics?), and then adding complexity only when needed.

Starting with a coarse modelling grid resolution and refining it as geological heterogeneity details are added to the modelling concept also saves significant computation time. While the geological concept gets refined, an important data curation effort may also be needed to fix potential data quality issues, for example well path depth or production allocation errors. Once the production history or simple a DST is bracketed by the initial ensemble, which means that the geological concept and uncertainty boundaries are well-defined and all data have been curated, an inverse data assimilation process edits the models until they match all the data, both static (well logs and 3D seismic), and dynamic (production and 4D seismic).

A physics-induced machine learning process, based on the Ensemble Kalman Smoother algorithm ***(adapted from Emerick and Reynolds, 2013)***,, is used to make local adjustments to all the models in the ensemble, which converges efficiently towards the observed data in a few iterations. Simulation results of the well test in the posterior ensemble simulations are highlighted in red on Figure 18.

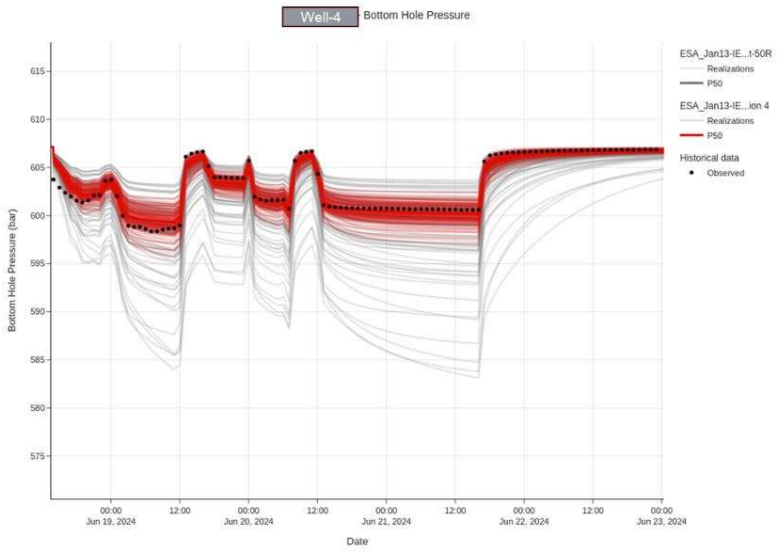

Figure 18:History matched ensemble in red, showing reasonable convergence towards the observed data

The analysis of the updates done by the Kalman Smoother algorithm supports the understanding of the reservoir characteristics, from structure to petrophysical properties and dynamic parameters, reducing uncertainties in the process. Figure 19 shows the changes done by the algorithm to the permeability in the vicinity of the well (within the red rectangle), consistently increasing it to yield lesser drawdown.

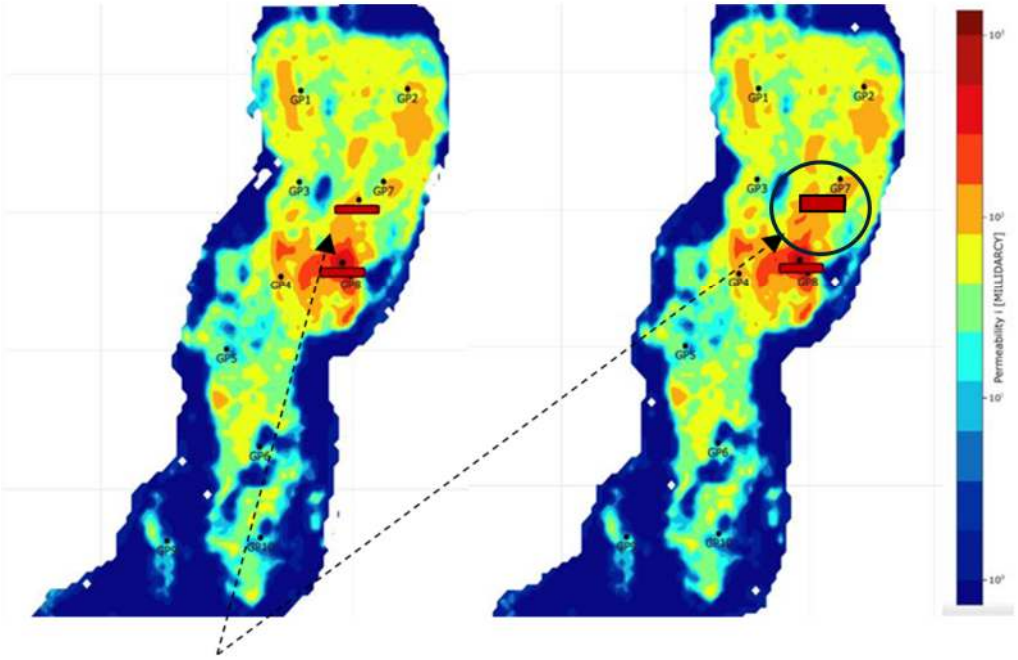

Figure 19:Aggregated ensemble permeability in the well region based on DST radius of investigation (Circle) – Prior ensemble on the left, posterior ensemble (after HM) on the right

Following calibration, the ensemble was used to establish connected volumes (Figure 20) and property filters are applied to identify target areas for well placement. These areas are identified probabilistically, by aggregation of the properties used in the ensemble, so as to highlight where gas saturation, porosity and permeability are consistently on the higher side throughout the 100 calibrated models.

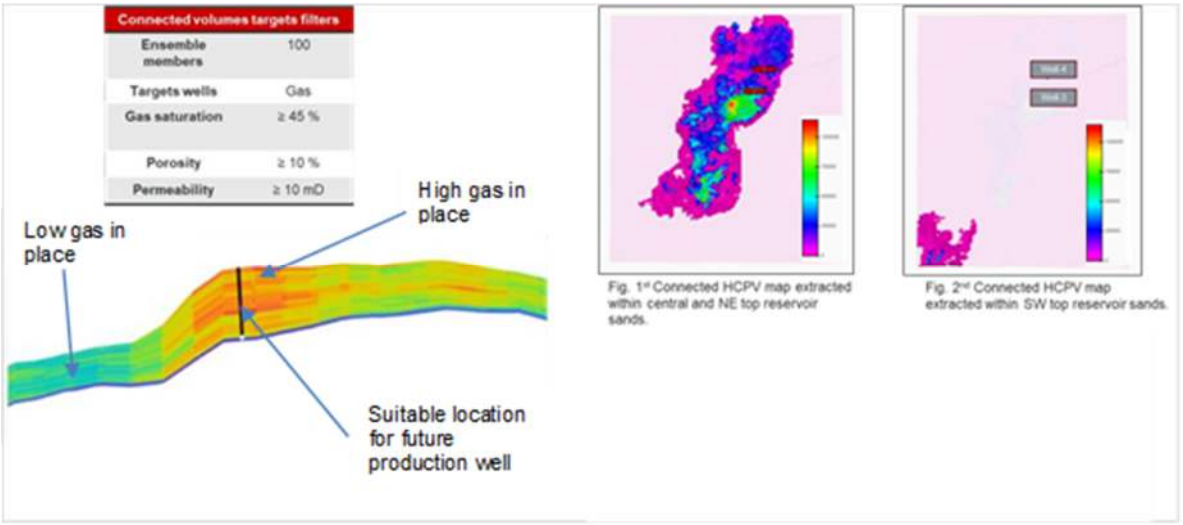

Figure 20:Infill well target placement based on aggregated ensemble statistics and filtering

A number of forecast scenarios were subsequently run to determine the potential outcome of operating the field and the expected ultimate recovery, while considering static and dynamic uncertainties.

Main operating assumptions are highlighted in

Figure ***21*** below and proposed well locations for one of the scenario displayed on the map.

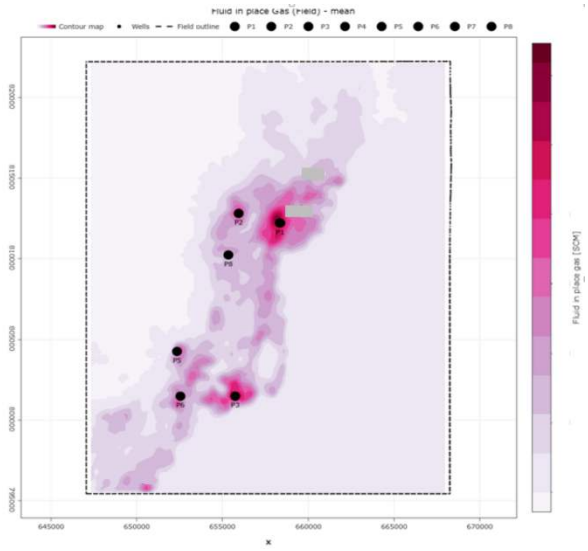

Figure 21:Forecast scenario rules and ensemble gas in place with possible well location (black dots) for one of the scenarios

Other scenarios considered the potential impact of a fault splitting the main channels into two parts. Figure 22 showcases how the production forecast varies between two different ensemble members (red and grey are both calibrated ensembles) depending whether the fault is sealing or fully open to flow, considering all other static and dynamic parameters as uncertain.

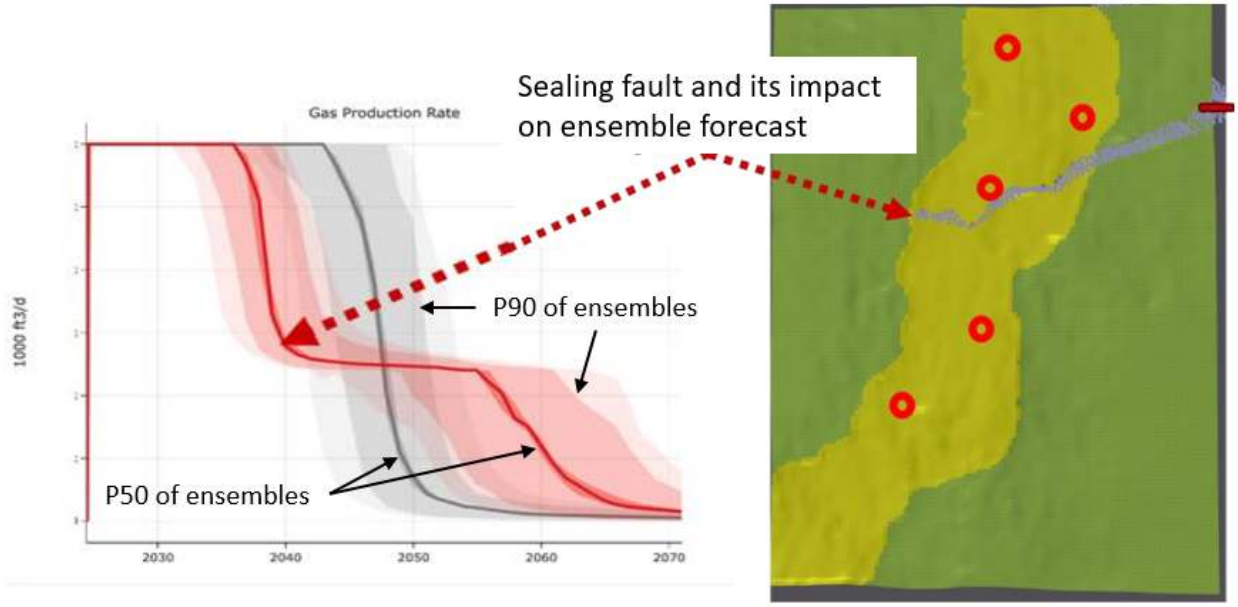

Figure 22:Impact of sealing fault on the field gas rate for one of the development scenario. Grey ensemble assumes the fault is open to flow while the red one assumes it is sealing. For both ensemble, the thicker line represents the statistical P50 of the ensemble

5. Results and Discussion

The integrated modeling workflow delivered measurable technical and business value across the exploration-to-development lifecycle. Most notably, the end-to-end cycle time was reduced by more than 50%, with the exploration-to-development handover shortened from approximately 18 months to about 6 months through the use of tightly coupled, iterative geoscience and reservoir-engineering workflows.

A robust chronostratigraphic framework was established using GTS 2020, allowing the extraction of 18 stratigraphic horizons over an area of approximately 9,500 km². The resulting horizon providing consistent and geologically meaningful sequence correlations based on 3rd – 4th order sequence boundaries across the study area and supporting multi-prospect integration.

Seismic resolution was significantly improved through the application of Sparse Layer Inversion (SLI). The inversion expanded the effective seismic bandwidth from approximately 10–40 Hz to 5–80 Hz, resulting in an estimated vertical resolution of ~8-10 m. This improvement enabled the identification of thin-bed geometries that were previously unresolved using conventional seismic products, directly enhancing reservoir architecture interpretation and stratigraphic detail.

The geological framework was implemented within a full-resolution, grid-less earth model. A point-cloud representation was used to preserve native well-log and seismic resolutions without averaging or upscaling, resulting in an earth model comprising approximately 100 million points. This model was visualized using volume-rendering techniques, enabling detailed interrogation of stratigraphy, facies architecture, and property distributions while maintaining computational efficiency.

Multivariate co-simulation based on pluri-gaussian modeling was applied to jointly model facies, porosity, and permeability distributions, with conditioning to seismic facies attributes. This approach effectively captured spatial heterogeneity and facies-controlled property relationships consistent with the depositional framework.

Uncertainty was quantified through a 100-realization ensemble of integrated reservoir models calibrated to DST data using an Ensemble Kalman Smoother (EnKS). This calibration reduced permeability uncertainty within the key pay interval by more than 40%, significantly improving confidence in dynamic behavior predictions . The calibrated ensemble delivered P0–P100 production forecasts constrained within ±15%, providing decision-grade probabilistic recovery envelopes suitable for development planning.

Connected volume analysis identified high-confidence well placement opportunities. Areas exhibiting greater than 80% connectivity across realizations were interpreted as low-risk targets for new producers. In addition, upside potential was identified in the southwest compartment, where more than 60% of realizations retained significant remaining gas volumes by 2070, indicating opportunities for future infill drilling .

Structural uncertainty was explicitly assessed through fault-sealing sensitivity analysis, quantifying its impact on production profiles and NPV-at-risk (Figure 21). The workflow further enabled flexible scenario testing, allowing multiple development strategies to be evaluated under uncertainty and compared on both technical and economic bases .

6. Conclusion

The implementation of an integrated, uncertainty-centric modeling approach proved to be highly efficient, reducing the overall project timeline by approximately 50%. The combination of sequence stratigraphic analysis with machine learning–assisted horizon interpretation enabled the construction of a regionally consistent geological framework across a 9,500 km² area encompassing multiple prospects, reducing interpretation time from several months to a matter of weeks.

Seismic resolution was improved by a factor of two through the application of a novel geophysical inversion technique, leading to enhanced characterization of reservoir architecture and facies distributions. The use of a single, grid-less, dynamically scalable earth and static model facilitated a seamless transition from exploration to development without the need for model rebuilding or resolution compromises.

Rapid generation of calibrated ensembles of integrated reservoir models allowed key subsurface uncertainties to be addressed efficiently and supported model-driven development planning and well placement decisions. As a result, the time required for dynamic modeling and history matching was reduced from several weeks to only a few days, significantly accelerating decision-making and improving overall project execution.

7. 7. Acknowledgements

The authors gratefully acknowledge PETRONAS Carigali Sdn. Bhd. for permission to publish this work and for their close technical collaboration throughout the study. The Subsurface and Consulting group at Halliburton

Malaysia provided critical expertise in seismic conditioning, stratigraphic interpretation, and reservoir modeling. The authors also acknowledge the Neftex® regional stratigraphy team for providing depositional element templates and GTS 2020 chronostratigraphic support. Ensemble-based modeling was supported by adaptive pluri-gaussian workflows and history-matching methodologies based on Ensemble Kalman Smoother techniques, developed through a combination of academic research and field-scale applications.

8. References

- Trude, J., Kilsdonk, B., Grow, T., & Ott, B. (2022c). The structure and tectonics of the Guyana Basin. *Geological Society London Special Publications*, *524*(1), 367–386. https://doi.org/10.1144/sp524-2021-117
- Alqallabi, S., Khan, A.S., Phade, A., Gacem, M.T., Adli, M., Al-Jenaibi, F., Manser, S., Maila, L. and Benedictis, D. [2021]. An Integrated Ensemble-Based Uncertainty Centric Approach to Address Multi-Disciplinary Reservoir Challenges While Accelerating Subsurface Modeling Process in an Onshore Field, Abu Dhabi, UAE. SPE205854-MS.
- Bratvold, R.B., Mohus, E., Petutschnig, D. and Bickel, D. [2020]. Production Forecasting: Optimistic and Overconfident — Over and Over Again. SPE Reservoir Evaluation and Engineering, 23(3), 0799-0810.
- Emerick, A.A. and Reynolds, A.C. [2013]. History-Matching Production and Seismic Data in a Real Field Case Using the Ensemble Smoother with Multiple Data Assimilation. Society of Petroleum Engineers. SPE-163675-MS.
- Panfili, P., Tveit, J.A., Sætrom, J., Halset, G. and Arrigoni, V. [2017]. Integrated Software Tool Brings Speed, Reliability to Reservoir Modeling on Barents Sea Project. Journal of Petroleum Technology, 40-2, April 2017.
- Strebelle, S., Hernandez, L. and Medina, R. [2023]. Scalable Earth Modeling: A Grid-less Multi-scale Multi-resolution Modeling Approach, 84th EAGE Conference and Exhibition, Vienna
- Zhang, R., & Castagna, J. (2011). Seismic sparse-layer reflectivity inversion using basis pursuit decomposition. Geophysics, 76(6), R147–R158. https://doi.org/10.1190/geo2011-0103.1
- Delhaye-Prat, V., Bourget, J., Gaillot, G., Gaillot, J., Sapin, F., Fillon, C., Ye, J., Wright, T., Chaboureau, A.-C., Buratti, N., Magnier, B., Belopolsky, A., Bez, M., Heumann, M. J.,
- Sullivan, M., Mathieu, J.-P., Cole, S., Ladner, B., Bull, J., & Dal, J.-A. (2024). Tectono- sedimentary evolution of the Suriname margin in the Cretaceous: A sequence-stratigraphic framework. Earth-Science Reviews, 253, 104770
- Gradstein, F. M., Ogg, J. G., Schmitz, M. D., & Ogg, G. M. (Eds.) (2020). Geologic Time Scale 2020 (2 vols.). Elsevier. ISBN 978-0-12-824360-2.